Biochimica et Biophysica Acta 1787 (2009) 1179–1188

Contents lists available at ScienceDirect

Biochimica et Biophysica Acta

journal homepage: www.elsevier.com/locate/bbabio

Identification and characterization of a cytochrome *b559 Synechocystis* 6803 mutant spontaneously generated from DCMU-inhibited photoheterotrophical growth conditions

Yi-Fang Chiu [a,b,c], Wen-Ching Lin [a], Chia-Ming Wu [a], Yung-Han Chen [d], Chung-Hsien Hung [a,e], Shyue-Chu Ke [d], Hsiu-An Chu [a,*]

[a] *Institute of Plant and Microbial Biology, Academia Sinica, Taipei, 11529, Taiwan*
[b] *Graduate Institute of Biotechnology, National Chung Hsing University, Taichung, 402, Taiwan*
[c] *Molecular and Biological Agricultural Sciences Program, Taiwan International Graduate Program, Academia Sinica, Taiwan*
[d] *National Dong-Hwa University, Hualien, 974-01, Taiwan*
[e] *Institute of Plant Biology, College of Life Science, National Taiwan University, Taipei 10617, Taiwan*

ARTICLE INFO

Article history:
Received 8 December 2008
Received in revised form 12 May 2009
Accepted 14 May 2009
Available online 21 May 2009

Keywords:
Photosystem II
Cytochrome *b559*
Photoinhibition
Chlorophyll *a* fluorescence
Site-directed mutagenesis
Synechocystis
EPR

ABSTRACT

We identified a spontaneously generated mutant from *Synechocystis* sp. PCC6803 wild-type cells grown in BG-11 agar plates containing 5 mM Glu and 10 μM DCMU. This mutant carries an R7L mutation on the α-subunit of cyt *b559* in photosystem II (PSII). In the recent 2.9 Å PSII crystal structural model, the side chain of this arginine residue is in close contact with the heme propionates of cyt *b559*. We called this mutant WR7Lα cyt *b559*. This mutant grew at about the same rate as wild-type cells under photoautotrophical conditions but grew faster than wild-type cells under photoheterotrophical conditions. In addition, 77 K fluorescence and 295 K chlorophyll *a* fluorescence spectral results indicated that the energy delivery from phycobilisomes to PSII reaction centers was partially inhibited or uncoupled in this mutant. Moreover, WR7Lα cyt *b559* mutant cells were more susceptible to photoinhibition than wild-type cells under high light conditions. Furthermore, our EPR results indicated that in a significant fraction of mutant reaction centers, the R7Lα cyt *b559* mutation induced the displacement of one of the axial histidine ligands to the heme of cyt *b559*. On the basis of these results, we propose that the Arg7Leu mutation on the α-subunit of cyt *b559* alters the interaction between the APC core complex and PSII reaction centers, which reduces energy delivery from the antenna to the reaction center and thus protects mutant cells from DCMU-induced photo-oxidative stress.

Photosystem II (PSII) is a multisubunit membrane protein complex in thylakoid membrane that functions as a water-plastoquinone oxidoreductase [1]. It utilizes light energy to oxidize water on the lumen side and to reduce plastoquinone on the stromal side of the thylakoid membrane. The major subunits of the PSII reaction center include D1, D2, CP43, CP47 and cyt *b559* [1–4]. D1 and D2 proteins constitute the core of the PSII reaction center. Nearly all redox cofactors which participate in the electron transfer reactions are bound to the D1/D2 protein core. CP43 and CP47 proteins bind chlorophyll molecules and serve as the PSII core antenna. Cytochrome (Cyt) *b559* is comprised of α and β subunits (encoded by the *psb*E and *psb*F genes) of 9 and 4 kDa, respectively [5]. Each subunit provides a His ligand for the non-covalently bound heme. In addition, cyt *b559* exhibits different redox potential forms: a high-potential (HP) form with a midpoint redox potential around +400 mV, an intermediate-potential (IP) form around +200–250 mV, and a low-potential (LP) form with a midpoint redox potential of about +50–100 mV ([5–9] and references therein). It has been proposed that the heme of cyt *b559* participates in a secondary electron transfer pathway that protects PSII from light-induced damage under photoinhibitory conditions ([5,10,11] and references therein) or functions as a PQ oxidase to keep the PQ pool oxidized [12–14]. Moreover, a novel quinone-binding site (Q_c) interacting with cyt *b559* in the PSII complex was proposed in recent studies [15,16] and was later identified in the new 2.9 Å PSII crystal structure [4]. The occupancy

Abbreviations: APC, allophycocyanin; Arg, arginine; Chl, chlorophyll *a*; cyt, cytochrome; DCBQ, 2,6-dichloro-p-benzoquinone; DCMU, 3-(3,4-dichloro-phenyl)-1,1-dimethylurea; Em, erythromycin; EPR, electron paramagnetic resonance; F_{eq}, steady-state fluorescence yield produced by weak monitoring flashes in the presence of DCMU; F_V/F_M, Maximum quantum yield of PSII; HP, high-potential; IP, intermediate-potential; Km, Kanamycin; PCR, polymerase chain reaction; PQ, plastoquinone; PSII, photosystem II; Pheo, primary pheophitin *a* electron acceptor; Q_A, the primary quinone electron acceptor in PSII; Q_B, the secondary quinone electron acceptor in PSII; LP, low-potential; wild-type*, control *Synechocystis* strain constructed in the same manner as cyt *b559* site-directed mutants but with no mutation

* Corresponding author. Tel.: +886 2 27871169; fax: +886 2 27827954.
E-mail address: chuha@gate.sinica.edu.tw (H.-A. Chu).

0005-2728/$ – see front matter © 2009 Elsevier B.V. All rights reserved.
doi:10.1016/j.bbabio.2009.05.007

of this Q_c site may modulate the redox equilibration between cyt *b559* and the PQ pool [15,16].

DCMU is an herbicide which binds to the Q_B-binding site in the PSII and thus inhibits forward electron transfer [17]. When the herbicide binding inhibits forward electron transfer, charge recombination can occur between $P680^+$Pheo radical pairs in the PSII reaction center and may result in formation of a chlorophyll triplet. This chlorophyll triplet is able to react with $^3O_2$, leading to singlet oxygen ($^1O_2$) formation [17–20]. $^1O_2$ can react with proteins, pigments and lipids and cause light-induced damage to PSII. In fact, previous studies suggest that the death of cells and of the plant might not be a result of starvation, but rather, due to herbicide-induced toxicity [18–20].

Synechocystis sp. PCC6803 is a unicellular non-nitrogen-fixing cyanobacterium. This strain has been used extensively for genetic studies of photosynthesis because it can grow photoheterotrophically on glucose and it is naturally transformable by exogenous DNA [21]. Previous studies have identified several spontaneously generated mutants from *Synechocystis* sp. PCC6803 cell grown photoautotrophically on solid BG-11 medium containing DCMU or other herbicides [22–24]. The amino acid side chains involved in herbicide resistance (herbicide binding) have been mapped in the region of D1 protein between 211 and 275 [22,23]. On the other hand, photoheterotrophical growth conditions (BG-11 medium containing 5 mM Glu and 10 μM DCMU) are often used for growing *Synechocystis* mutant cells with impaired photosynthetic activity, to prevent mutant cells from reverting back to wild-type cells. However, so far there has been no report on the effect of DCMU-induced photo-oxidative stress on *Synechocystis* sp. PCC6803 cells grown under photoheterotrophical conditions.

Here we identify and characterize one spontaneously-occurring mutant from *Synechocystis* sp. PCC6803 wild-type* cells, grown in BG-11 agar plates containing 5 mM Glu and 10 μM DCMU.

1. Materials and methods

1.1. Growth and preparation of Synechocystis sp. PCC6803 cells

Synechocystis cells were propagated in BG-11 medium alone for photoautotrophical growth conditions or in BG-11 medium supplemented with 5 mM glucose and 10 μM DCMU for photoheterotrophical growth conditions. Cultures were propagated at 30 °C under a light intensity of 25–30 μmol photons m^{-2} s^{-1} and were continuously bubbled with sterile, humidified air.

1.2. Construction of R7Lα cyt b559 mutants

The R7Lα mutation was introduced into the plasmid PAC559EM^R by oligonucleotide-derived mutagenesis according to reference [25]. The R7Lα cyt *b559* mutant was constructed by transformation of the mutant plasmid into the host strain (Δ*psb*EFLJ) [25]. Mutants were selected on solid media containing the antibiotic Em (0.1 μg/mL) until their mutated gene was completely segregated. Complete segregation of the mutated gene in these mutant cells was verified by PCR [25].

1.3. Measurement of photosynthetic oxygen-evolution

Concentrated cells were diluted into growth medium held at 25 °C in a stirred, water-jacketed cell. Two millimolar potassium ferricyanide and 2 mM 2,6-dichloro-p-benzoquinone (DCBQ) were added to the medium immediately prior to the addition of the cells. Steady-state rates of oxygen-evolution were measured with a Clark-type oxygen electrode (YSI model 5331 oxygen probe) fitted with a water-jacketed cell. Saturating illumination was provided from both sides of the water-jacketed cell by two fiber-optic illuminators (Dolan-Jenner model MI 150).

1.4. Measurement of chlorophyll a fluorescence at 295 K

Chlorophyll *a* fluorescence measurements at 295 K were performed with a Dual PAM (pulse-amplitude-modulation) fluorometer (Walz, Germany). The relative PSII content of cells on a chlorophyll basis was estimated from the total yield of variable chlorophyll *a* fluorescence ($F_{max} - F_0$) measured in the presence of DCMU and hydroxylamine, according to the references [25–27]. Experimental conditions for measurements of fluorescence induction and recovery, the kinetics of charge recombination between Q_A^- and PSII electron donors, and electron transfer from Q_A^- to Q_B in response to a saturating flash given to wild-type and mutant cells are described in the figure legends.

1.5. Measurement of fluorescence at 77 K

Fluorescence emission spectra were recorded with a fluorescence spectrometer (Jasco model FP-6500). All the measurements were carried out at 77 K, using cell suspensions at a chlorophyll concentration of 20 μg/ml. The excitation light wavelength used for exciting chlorophyll was 435 nm (excitation band width 5 nm, emission band width 1 nm). The excitation light wavelength used for phycobilisomes was 600 nm (excitation band width 3 nm, emission band width 1 nm).

1.6. Preparations of His-tagged PSII core complexes

Oxygen-evolving His-tagged PSII core complexes were isolated by Ni-NTA affinity chromatography from wild-type WR7Lα and R7Lα mutant cells, which contain a His-tag on their CP47 proteins, as described in the reference [25]. The oxygen activity for wild-type WR7Lα and R7Lα mutant PSII core complexes was about 2100, 1770, and 980 μmol of O_2/mg of Chl per hour, respectively. Tris-washed samples were prepared, in accordance with the references cited [25].

1.7. Reduced minus oxidized difference spectra of cyt b559 in wild-type and mutant PSII core complexes

Optical absorption difference measurements were performed on suspensions of wild-type* and mutant PSII core complexes (20 μg/ml Chl) in 1 ml MMNB buffer (25 mM Mes, 5 mM $MgCl_2$, 10 mM NaCl, 1 M glycine betaine, 0.03% DM, pH 5.7) at room temperature, on a Jasco V-560 UV/VIS spectrophotometer with band width of 1.0 nm. Four-step redox titration was performed, as described in the reference [14]. The sample suspension was oxidized by adding 0.1 mM $K_3Fe(CN)_6$ (from a fresh made 10 mM stock solution) and the spectrum was recorded and stored as the oxidized spectrum. The reduction was performed by first adding hydroquinone (0.3 mM), followed by ascorbate (0.6 mM) and, finally, a few grains of dithionite.

1.8. Conditions for EPR measurements

EPR spectra were obtained at X-band using a Bruker EMX spectrometer equipped with a Bruker TE102 cavity and an Advanced Research System continuous-flow cryostat (3.2 K–200 K). The microwave frequency was measured with a Hewlett-Packard 5246L electronic counter. The instrument settings are shown in the figure legend.

2. Results

2.1. Identification of a spontaneously generated Synechocystis sp. PCC6803 mutant

We identified one spontaneously generated mutant from *Synechocystis* sp. PCC6803 wild-type* cells grown in BG-11 medium

containing 5 mM Glu and 10 μM DCMU at a light intensity of about 30 μmol photons m^{-2} s^{-1}. We sequenced the entire coding regions of PsbA (encodes D1 protein), PsbD (encodes D2), PsbB (encodes CP47), PsbC (encodes CP43) and PsbEFLJ genes (encode cyt *b559*α and β, PsbL and PsbJ proteins) of this mutant. We found that this mutant carried an Arg to Leu mutation on the 7th amino acid residue of the α-subunit of cyt *b559*. In addition, we also found that this mutated gene was completely segregated in the genomes of mutant cells. We call this mutant WR7Lα cyt*b559*. To confirm that the R7L mutation on the α subunit of cyt *b559* is responsible for the phenotypes that we observed in the WR7Lα mutant, we also constructed an R7Lα cyt *b559* mutant by site-directed mutagenesis.

2.2. Oxygen-evolution activity, PSII contents and growth characteristics of mutant cells

The light-saturated oxygen-evolution activity and PSII contents of the mutant strains are listed in Table 1. The oxygen-evolving rates of WR7Lα and R7Lα cyt *b559* mutant cells were both about 70% compared to that of wild-type cells. The PSII content of WR7Lα and R7Lα cyt *b559* mutant cells were 90 ± 6% and 84 ± 2%, respectively, compared to wild-type cells. In addition, WR7Lα cyt *b559* mutant cells grew at about the same rate as wild-type cells under photoautotrophical conditions (in BG-11 medium). In contrast, WR7Lα cyt *b559* mutant cells grew faster than wild-type cells under photoheterotrophical conditions (in BG-11 medium containing 5 mM Glu and 10 μM DCMU). The doubling time of WR7Lα and R7Lα cyt *b559* mutant and wild-type cells under these photoheterotrophical growth conditions were about 16.9, 18.2, and 22.0 h, respectively (see Table 1).

2.3. PSII fluorescence yield in the presence and absence of actinic light

WR7Lα cyt *b559* mutant cells showed very distinct time-dependent, flash-induced transients of fluorescence yield in the presence and absence of actinic light compared to wild-type cells (see Fig. 1). The F_0 (~0.19) is higher and the $F_V/F_{M,dark}$ value (~0.30) is lower in the spectrum of WR7Lα cyt *b559* mutant cells (red trace) than the F_0 (~0.11) and $F_V/F_{M,dark}$ value (~0.41) in the spectrum of wild-type cells (blue trace). In addition, the maximum fluorescence (F_M) in WR7Lα cyt *b559* mutant cells was significantly increased during actinic light illumination and then decreased while the actinic light was turned off. In contrast, the F_M value in wild-type cells was almost constant before, during and after the actinic light illumination. The high F_0 value and the increase of the F_M value during actinic light illumination could be due to increased fluorescence emission from uncoupled phycobilisomes in WR7Lα cyt *b559* mutant cells. Furthermore, in WR7Lα cyt *b559* mutant cells (Fig. 1, red trace), the F_V/F_M value (down to ~0.18) after actinic light illumination is significantly lower than the $F_V/F_{M,dark}$ values (~0.30). In contrast, in wild-type cells (Fig. 1, blue trace), the F_V/F_M value after actinic light illumination is about the same as the $F_V/F_{M,dark}$ value (~0.41). These results suggest that WR7Lα cyt *b559* mutant cells suffer from photoinhibition during actinic light illumination.

Table 1
Summary of properties of cyt *b559* mutant cells.

Strains	O_2 evolution (% wild-type)	PSII content (% of wild-type)	Doubling time for photoheterotrophic growth (hours)
Wild-type	100 ± 7	100 ± 5	22.0 ± 1.0
WR7Lα	70 ± 5	90 ± 6	16.9 ± 0.3
R7Lα	69 ± 13	84 ± 2	18.2 ± 0.1

Experimental conditions are described in materials and methods. The average O_2 evolution rate of wild-type cells was 440 ± 87 μmol O_2/mg Chl × hour. The average variable fluorescence yield of wild-type cells was 0.39 ± 0.06.

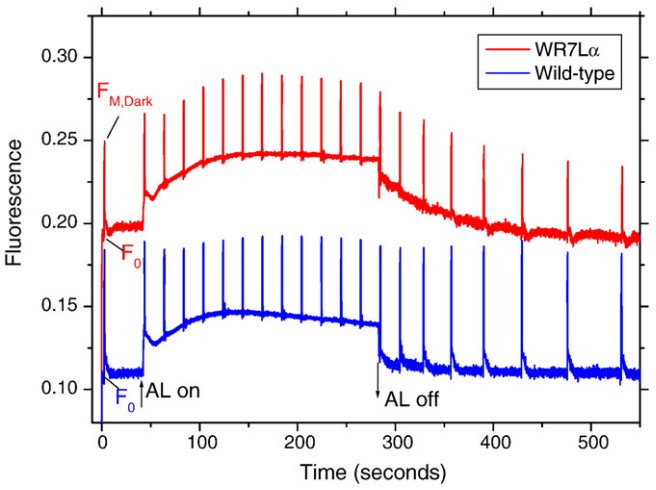

Fig. 1. Time-dependent flash-induced transients of fluorescence yield of wild-type (blue trace) and WR7Lα cyt *b559* mutant cells (red trace) in the presence and absence of actinic light. Conditions: 20 μg of Chl in 2 mL of BG11 medium at 295 K. Samples were incubated in darkness for 5 min. The intensity of the actinic light is about 38 μmol photons m^{-2} s^{-1}.

2.4. Measurement of chlorophyll a fluorescence at 295 K

Fig. 2 shows the induction and decay of chlorophyll *a* fluorescence in response to a saturating flash delivered to wild-type, WR7Lα and R7Lα cyt *b559* mutant cells in the presence of 40 μM DCMU. The decay of chlorophyll *a* fluorescence in the presence of DCMU is due mostly to the charge recombination between Q_A^- and PSII electron donors. The kinetics of charge recombination between Q_A^- and PSII electron donors is sensitive to the presence or absence of photooxidizable Mn ions and the redox potential of Q_A^- in PSII [26,28]. Because WR7Lα and R7Lα cyt *b559* mutant cells show very similar kinetics of chlorophyll *a* fluorescence decay to that in wild-type cells, our results suggest that the Mn cluster and Q_A were intact in WR7Lα and R7Lα cyt *b559* mutant cells. Furthermore, the flash-induced yields of variable chlorophyll *a* fluorescence in WR7Lα and R7Lα were about 1.1 fold

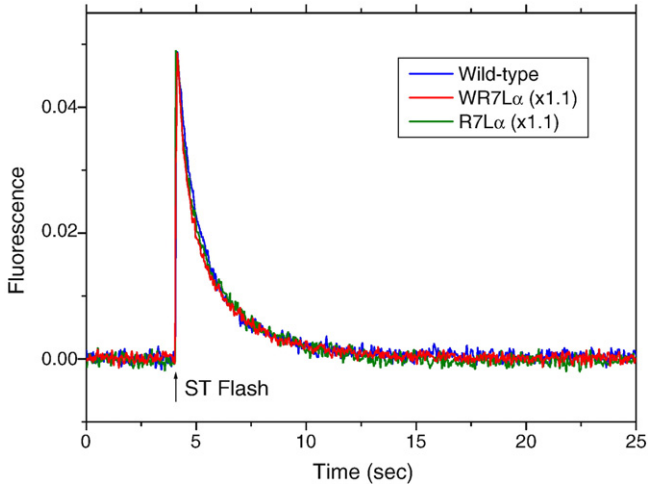

Fig. 2. The kinetics of charge recombination between Q_A^- and PSII electron donors in response to a saturating flash given to wild-type (blue trace), WR7Lα (red trace) and R7Lα cyt *b559* mutant cells (green trace) in the presence of DCMU, by chlorophyll *a* fluorescence measurement. Conditions: 20 μg of Chl in 1 mL of BG-11 medium. Samples were incubated in darkness for 1 min before DCMU was added to the final concentration of 40 μM. The F_{eq} value for wild-type (blue trace), WR7Lα (red trace) and R7Lα cyt *b559* mutant cells (green trace) is 0.13, 0.20, and 0.20, respectively.

lower than that of wild-type* cells (see Fig. 1). These slightly lowered yields in the mutant cells were roughly correlated with their lower PSII contents compared to wild-type cells (Table 1). Fig. 3 shows the induction and decay of Q_A^- in response to a saturating flash in the absence of DCMU. Fluorescence decay in the absence of DCMU is due mostly to forward electron transfer from Q_A^- to Q_B and Q_B^-. Our results show that the electron transfer rate from Q_A^- to Q_B and Q_B^- in WR7Lα and R7Lα cyt *b559* mutant cells is slightly slower than in wild-type cells.

2.5. Susceptibility to photoinhibition

Fig. 4 shows effects of photoinhibition on the PSII activity of wild-type, WR7Lα and R7Lα cyt *b559* mutant cells. Our results show that the PSII activities in WR7Lα and R7Lα cyt *b559* mutant cells decreased much faster than in wild-type cells under high light conditions. Therefore, WR7Lα and R7Lα cyt *b559* mutant cells were more susceptible to photoinhibition than wild-type cells under high light conditions.

2.6. Redox-induced optical absorption difference spectra of the cyt b559 heme

To facilitate the isolation of PSII core complexes, we constructed WR7Lα and R7Lα cyt *b559* mutant strain that contains a hexahistidine-tag (His-tag) fused to the C-terminus of CP47 [25]. The dithionite-reduced minus ferricyanide-oxidized difference spectra of the cyt *b559* heme in His-tagged PSII core complexes isolated from this WR7Lα cyt *b559* mutant strain are shown in Fig. 5. WR7Lα cyt *b559* mutant PSII core complexes (black trace) gave rise to dithionite-reduced minus ferricyanide-oxidized difference spectra that can be attributed to redox-induced absorption changes of cyt *b559* and cyt *c550*. On the other hand, difference spectra from Tris-washed WR7Lα cyt *b559* PSII core complexes (green trace) [that were depleted of Mn ions and extrinsic polypeptides, including cyt *c550*] showed the maximum absorption at around 559.5 nm, attributable to redox-induced absorption changes in cyt *b559*. In addition, our results indicated that the amplitude of the absorption of cyt *b559* in WR7Lα mutant PSII core complexes was about 80% of that in wild-type PSII core complexes (see reference [25]). The decrease of the cyt *b559* content in WR7Lα mutant PSII core complexes is correlated with the decrease of the PSII content in WR7Lα mutant cells (see Table 1). On the basis of these results, we conclude that WR7Lα mutant PSII core complexes retain the heme of cyt *b559*. Furthermore, our results also showed that Tris-washed WR7Lα cyt *b559* mutant PSII core complexes did not significantly modify the maximum absorption of cyt *b559* (in Fig. 5, green trace).

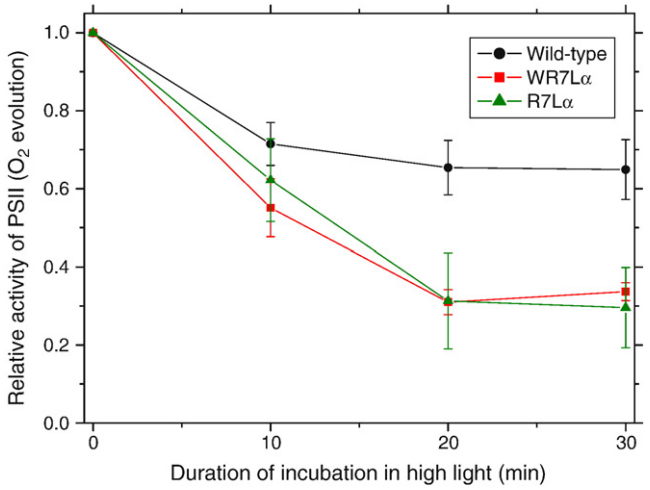

Fig. 4. Effects of photoinhibition on PSII activity (oxygen-evolution) of wild-type (black trace), WR7Lα (red trace) and R7Lα cyt *b559* mutant cells (green trace) under high light conditions. Cells were incubated in BG-11 medium (20 mg of Chl/ml) at ~2500 μmole photons m^{-2} s^{-1}. The oxygen-evolution activity of wild-type (black trace), WR7Lα cyt (red trace) and R7Lα cyt *b559* mutant cells (green trace) at time 0 were 477 ± 46, 354 ± 44, and 371 ± 72, respectively.

2.7. Effect of DCMU concentrations on the oxygen-evolving activity

Fig. 6 shows the effect of the DCMU concentration on the oxygen-evolving activity of wild-type, WR7Lα and R7Lα cyt *b559* mutant cells. Our results showed that the DCMU concentration had the same inhibitory effect on oxygen-evolving activity of wild-type, WR7Lα and R7Lα cyt *b559* mutant cells. In addition, the concentration of DCMU

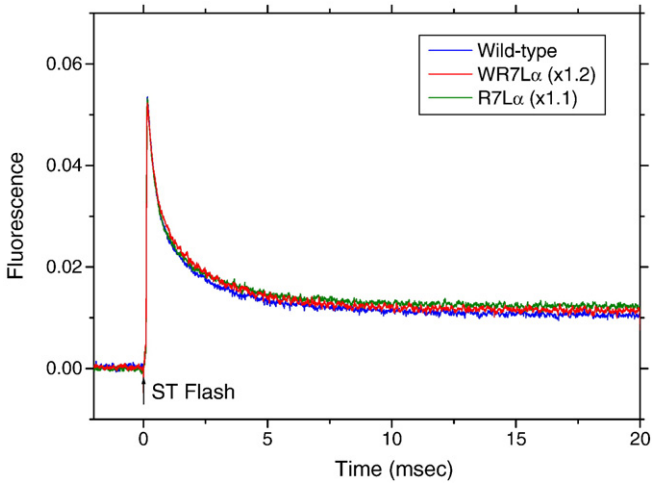

Fig. 3. The kinetics of electron transfer from Q_A^- to Q_B and Q_B^- in response to a saturating flash given to wild-type (blue trace), WR7Lα (red trace) and R7Lα cyt *b559* mutant cells (green trace), by chlorophyll *a* fluorescence measurement. Conditions: 20 μg of Chl in 1 mL of BG-11 medium. Samples were incubated in darkness for 1 min. The F_0 value for wild-type (blue trace), WR7Lα (red trace) and R7Lα cyt *b559* mutant cells (green trace) is 0.11, 0.19, and 0.19, respectively.

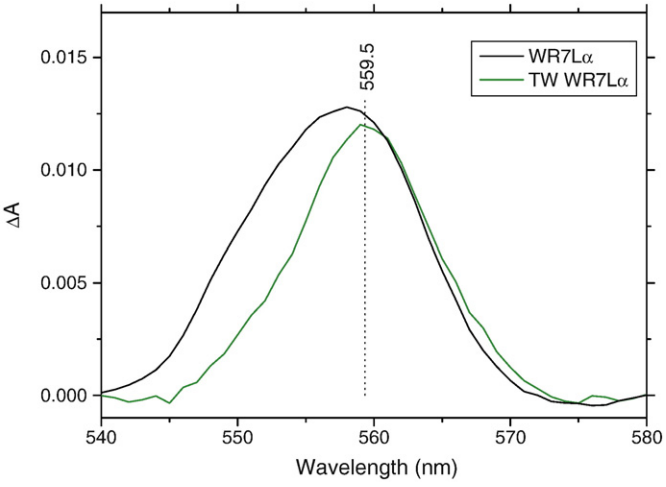

Fig. 5. The dithionite-reduced minus ferricyanide-oxidized difference spectra of cyt *b559* heme in WR7Lα cyt *b559* mutant PSII core complexes. Spectra of untreated and Tris-washed (TW) WR7Lα cyt *b559* mutant PSII core complexes are in black and green, respectively. The measurement was performed at room temperature. A linear baseline correction has been applied to each difference spectrum that consists of a straight line connecting the spectral values at 540 and 580 nm.

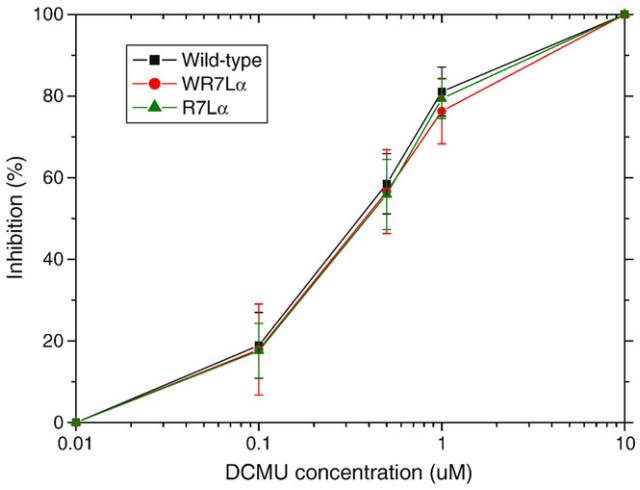

Fig. 6. Effects of DCMU concentration on the oxygen-evolving activity of wild-type (black trace), WR7Lα (red trace) and R7Lα cyt *b559* mutant cells (green trace). The oxygen-evolving activity of wild-type (black trace), WR7Lα (red trace) and R7Lα cyt *b559* mutant cells (green trace) in the absence of DCMU were 440 ± 16, 328 ± 53 and 314 ± 35, respectively.

that produced 50% inhibition of the oxygen-evolving activity was about the same (~0.4 μM) for wild-type, WR7Lα and R7Lα cyt *b559* mutant cells (see Fig. 6).

2.8. 77 K fluorescence emission spectra

Fig. 7A shows the 77 K fluorescence emission spectra recorded from cells that were excited at 600 nm, where the phycobilin pigments preferentially absorb. In spectra of wild-type cells, fluorescence peaks at ~660 nm originating from allophycocyanin and a peak at ~690 nm originating from photosystem II. In spectra of WR7Lα cyt *b559* mutant cells, a fluorescence peak was present at ~660 nm but the other peak was strongly enhanced and shifted to 686 nm. The emission peak at ~686 nm originated from terminal phycobilin emitters (ApcE) or from CP43 [29–32]. Therefore, the strong enhancement of emission peaks at 686 nm in WR7Lα cyt *b559* mutant cells indicated that the energy transfer from phycobilisomes to PSII reaction centers were partially inhibited or uncoupled in these mutant cells.

Fig. 7B shows the 77 K fluorescence emission spectra recorded from cells excited at 435 nm, where the chlorophyll molecule preferentially absorbs. In spectra of wild-type and WR7Lα cyt *b559* mutant cells, preferential excitation of chlorophyll at 435 nm resulted in three emission peaks: at ~685, ~694 and ~720 nm. According to previous studies, the emission peak at ~685 nm originate from CP43 or from terminal phycobilin emitters (ApcE) [30–33], whereas the origin of the emission peak at ~694 nm seems to originate from CP47 functionally coupled to the PSII reaction center. The emission peak at ~720 nm originates from Chl *a* in PSI ([30–33] and references therein). Therefore, the slightly lower intensity at ~694 nm in the WR7Lα cyt *b559* mutant spectrum compared to the wild-type spectrum was correlated with PSII content. In addition, the significantly enhanced emission at ~685 nm in the mutant spectrum can be attributed to partially uncoupled phycobilisomes in WR7Lα cyt *b559* mutant cells. Furthermore, the ratio of the amplitude of PSI peak at 720 nm over the amplitude of PSII peak at 695 nm (about 1.5) in spectra of wild-type cells under DCMU-inhibited growth conditions (Fig. 7B, blue trace) is significantly lower than the ratio of that (about 2.0) under normal growth condition [25]. Therefore, our results suggest that the PSI to PSII ratio in wild-type cells is significantly decreased under DCMU-inhibited growth conditions.

2.9. Determination of different potential forms of cyt b559 in wild-type and mutant PSII core complexes

To estimate the potential forms of cyt *b559* in wild-type and mutant PSII core complexes, we measure reduced minus oxidized optical difference spectra of the cyt *b559* heme in (A) wild-type, (B) WR7Lα, and (C) R7Lα cyt *b559* mutant oxygen-evolving PSII core complexes using four-step titration (ferricyanide → hydroquinone → ascorbate → dithionite) (Fig. 8). A hydroquinone-reduced minus fericyanide-oxidized absorption difference spectrum (HF, green trace) was used to estimate the HP form of cyt *b559*, and an ascorbate-reduced minus hydroquinone-oxidized absorption difference spectrum (AH, blue trace) was used to estimate the IP form of cyt *b559*. Dithionite-reduced minus ascorbate-oxidized absorption difference spectrum (DA, red trace) of cyt *b559* contains both the LP form of cyt *b559* and cyt *c550*. Because cyt *c550* does not contribute significantly at 559.5 nm of the difference spectrum [7,34], therefore, we used the amplitude of dithionite-reduced minus ascorbate-oxidized absorption difference spectra at 559.5 nm to estimate the amount of the LP form of cyt *b559*. Our results showed that oxygen-evolving wild-type PSII core

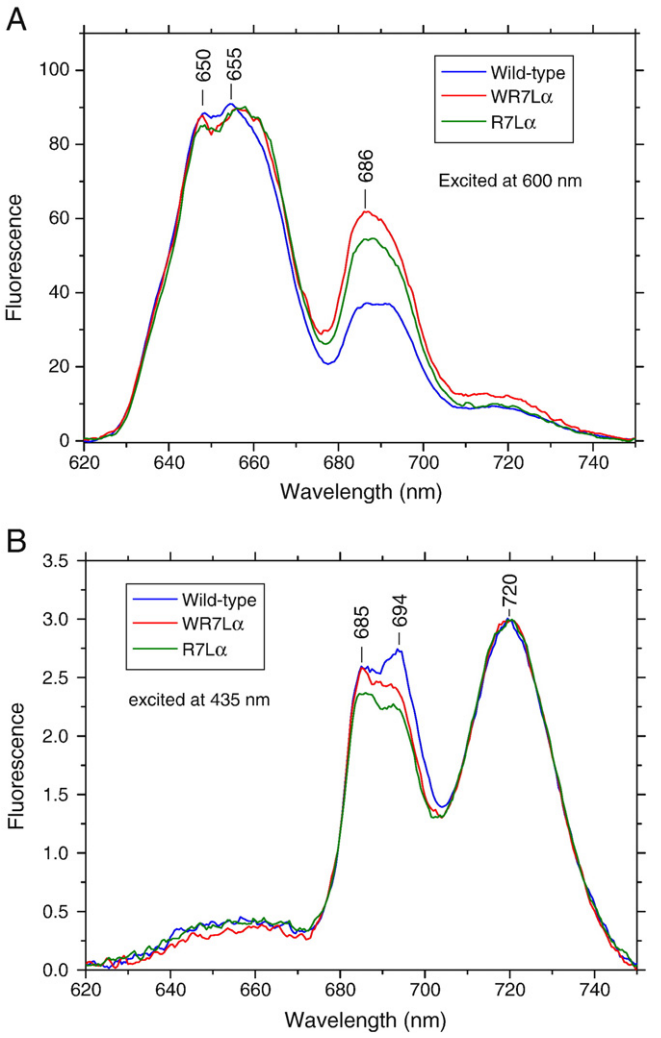

Fig. 7. 77 K-fluorescence emission spectra from wild-type (blue trace) and WR7Lα cyt *b559* mutant cells (red trace) grown under photoherterotrophical conditions. (A) excited phycoblisomes at 600 nm (excitation bandwidth 3 nm; emission bandwidth 1 nm; spectra were normalized at 660 nm) and (B) excited chlorophyll at 435 nm (excitation bandwidth 5 nm; emission bandwidth 1 nm; spectra were normalized at 720 nm). All measurements were carried out at 77 K, using cell suspensions at a chlorophyll concentration of 20 μg/mL.

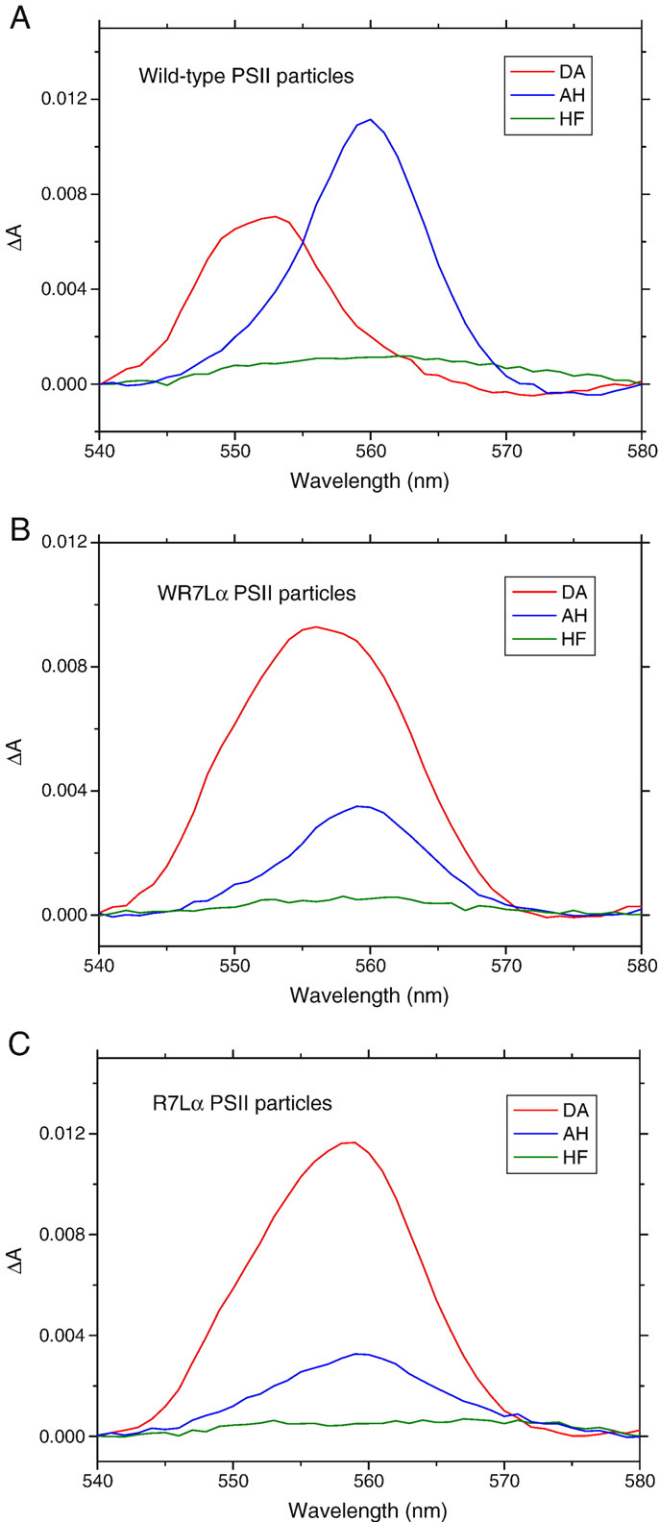

Fig. 8. The reduced minus oxidized difference spectra of cyt *b559* heme in oxygen-evolving (A) wild-type, (B) WR7Lα, and (C) R7Lα cyt *b559* mutant PSII core complexes. DA: the dithionite-reduced minus ascorbate-oxidized difference spectrum (red trace); AH: the ascorbate-reduced minus hydroquinone-oxidized difference spectrum (blue trace); HF: the hydroquinone-reduced minus ferricyanide-oxidized difference spectra (green trace). A linear baseline correction has been applied to each difference spectrum that consists of a straight line connecting the spectral values at 540 and 580 nm.

Table 2
Content of HP, IP, LP forms of cyt *b559* (in % of total Cyt *b559*, ± 7%) in wild-type and cyt *b559* mutant PSII core complexes.

Strains	PSII samples	Redox forms		
		HP	IP	LP
Wild-type	O_2 evolving	8%	78%	14%
	Tris-washed	11%	59%	30%
WR7Lα	O_2 evolving	4%	28%	68%
	Tris-washed	0%	35%	65%
R7Lα	O_2 evolving	3%	22%	75%
	Tris-washed	8%	29%	63%

complexes contain ~8% HP form, ~78% IP form and ~14% LP form of cyt *b559*. In contrast, WR7Lα (Fig. 8A) and R7Lα cyt *b559* mutant PSII core complexes (Fig. 8B) contain more LP form (~68% and 75%, respectively), less IP form (~28% and ~22%, respectively) and little HP form of cyt *b559* (see Table 2). In addition, Fig. 9 shows reduced minus oxidized optical difference spectra of the cyt *b559* heme in Tris-washed (A) wild-type, (B) WR7Lα, and (C) R7Lα cyt *b559* mutant PSII core complexes, using the four-step titration. Because Tris-washed wild-type and mutant PSII core complexes were depleted of Mn ions and extrinsic polypeptides (including cyt *c550*), their dithionite-reduced minus ascorbate-oxidized absorption difference spectra (DA, red trace) of cyt *b559* contain only the LP form of cyt *b559*. Our results showed that Tris-washed wild-type PSII core complexes contain 11% HP form, 59% IP form and 30% LP form of cyt *b559* (see Fig. 9A). The amount of the LP form of cyt *b559* in Tris-washed wild-type PSII core complexes (Fig. 9A) was increased about 15% at the expense of the IP form compared to spectra of oxygen-evolving wild-type PSII core complexes (Fig. 8A). In contrast, the amount of the LP form of cyt *b559* in Tris-washed, WR7Lα and R7Lα cyt *b559* mutant PSII core complexes (Fig. 9B and C) did not show any significant change.

2.10. CW-EPR spectra of wild-type and mutant PSII core complexes

Fig. 10 shows CW-EPR spectral characterizations of cyt *b559* from oxygen-evolving (A) wild-type, (B) WR7Lα, and (C) R7Lα cyt *b559* mutant PSII core complexes. Wild-type PSII core complexes gave rise to EPR signals which are characteristic for the low-spin heme of cytochromes ($g_z = 2.92$; $g_y = 2.26$) contributed from both cyt *b559* and cyt *c550*. In contrast, WR7Lα and R7Lα cyt *b559* mutant PSII core complexes gave rise to EPR signals which are characteristic for both the low-spin heme of cytochromes ($g_z = 2.93$; $g_y = 2.26$; from both LP form of cyt *b559* and cyt *c550*) and also the high-spin heme of cyt *b559* ($g_z = 6.10$; $g_y = 5.88$) (35). In addition, under 77 K illumination, wild-type and WR7Lα PSII core complexes (Fig. 10A and B, blue trace) gave rise to additional EPR signals ($g_z = 3.05$; $g_y = 2.17$) which were contributed from photo-oxidization of HP and some IP form of cyt *b559*. Fig. 11 shows CW-EPR spectral characterizations of cyt *b559* from Tris-washed (A) wild-type, (B) WR7Lα, and (C) R7Lα mutant PSII core complexes. Tris-washed wild-type PSII core complexes gave rise to EPR signals which are characteristic for the low-spin heme of cyt *b559* ($g_z = 2.98$; $g_y = 2.25$). In contrast, Tris-washed WR7Lα and R7Lα cyt *b559* mutant PSII core complexes gave rise to EPR signals which are characteristic for both the low-spin heme of cyt *b559* ($g_z = 2.95$; $g_y = 2.26$) and the high-spin heme of cyt *b559* ($g_z = 6.10$; $g_y = 5.88$).

3. Discussion

In this study, we identified a spontaneously generated WR7Lα cyt *b559* mutant from wild-type cells grown in BG-11 containing 5 mM Glu and 10 μM DCMU. Our results showed that the oxygen-evolving activity, PSII content, growth characteristics, 77 K fluorescence and 295 K chlorophyll *a* fluorescence spectral results, susceptibility to photoinhibition, and the DCMU effect on the oxygen-evolving activity

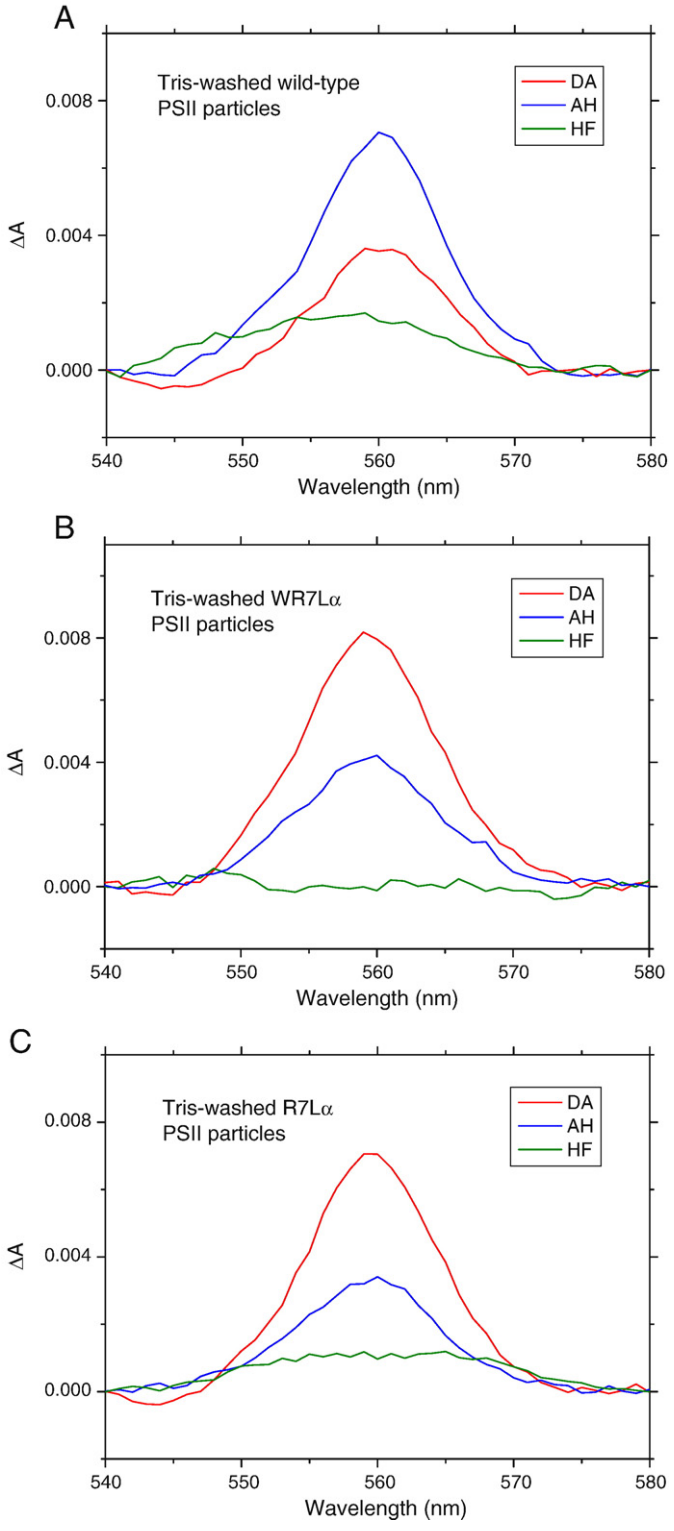

Fig. 9. The reduced minus oxidized difference spectra of cyt *b559* heme in Tris-washed (A) wild-type, (B) WR7Lα, and (C) R7Lα cyt *b559* mutant PSII core complexes. DA: the dithionite-reduced minus ascorbate-oxidized difference spectrum (red trace); AH: the ascorbate-reduced minus hydroquinone-oxidized difference spectrum (blue trace); HF: the hydroquinone-reduced minus ferricyanide-oxidized difference spectra (green trace). A linear baseline correction has been applied to each difference spectrum that consists of a straight line connecting the spectral values at 540 and 580 nm.

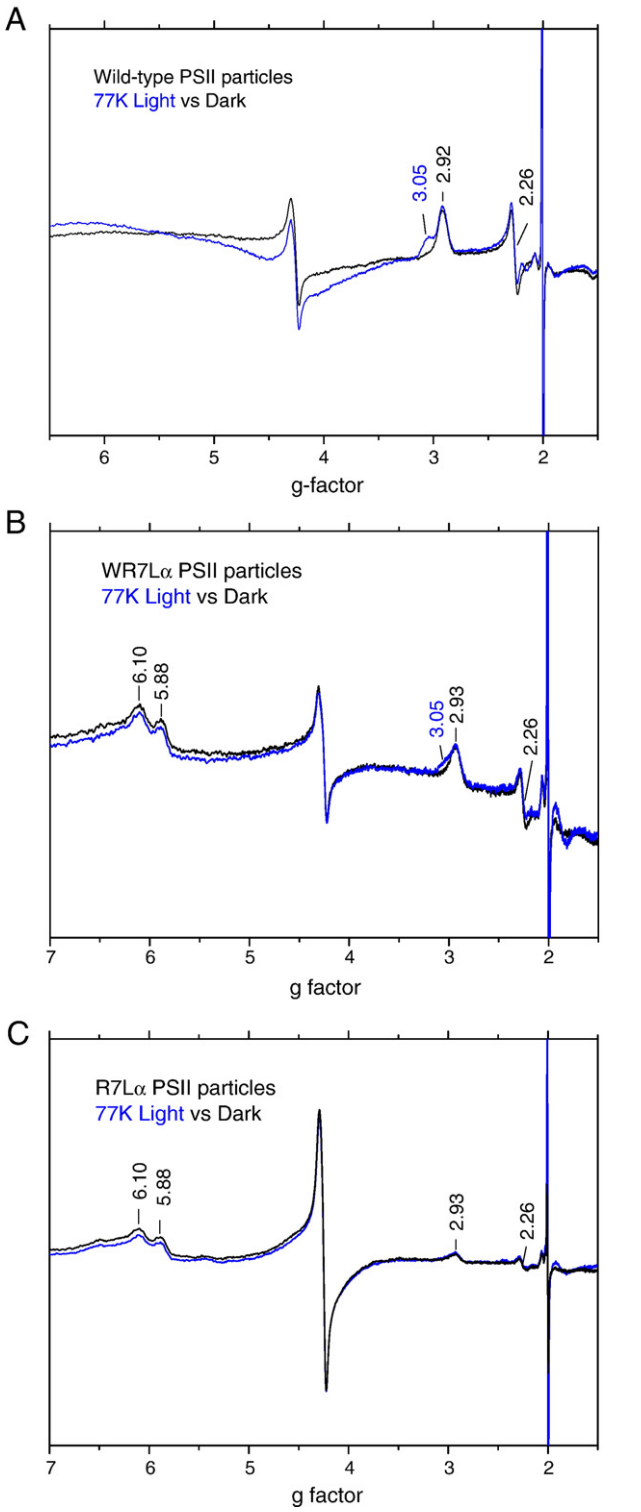

Fig. 10. The EPR spectra of cyt *b559* heme in oxygen-evolving (A) wild-type, (B) WR7Lα, and (C) R7Lα cyt *b559* mutant PSII core complexes. Spectra of dark adapted samples and following 77 K illumination are in black and blue colors, respectively. EPR conditions: microwave frequency, 9.54 GHz; modulation amplitude, 20 G at 100KHz; temperature, about 10 K; microwave power, 20 mW.

of WR7Lα cyt *b559* mutant cells were very similar to those in site-directed R7Lα cyt *b559* mutant cells. Therefore, we conclude that the R7Lα cyt *b559* mutation is responsible for the distinct phenotypes we observed in WR7Lα cyt *b559* mutant cells.

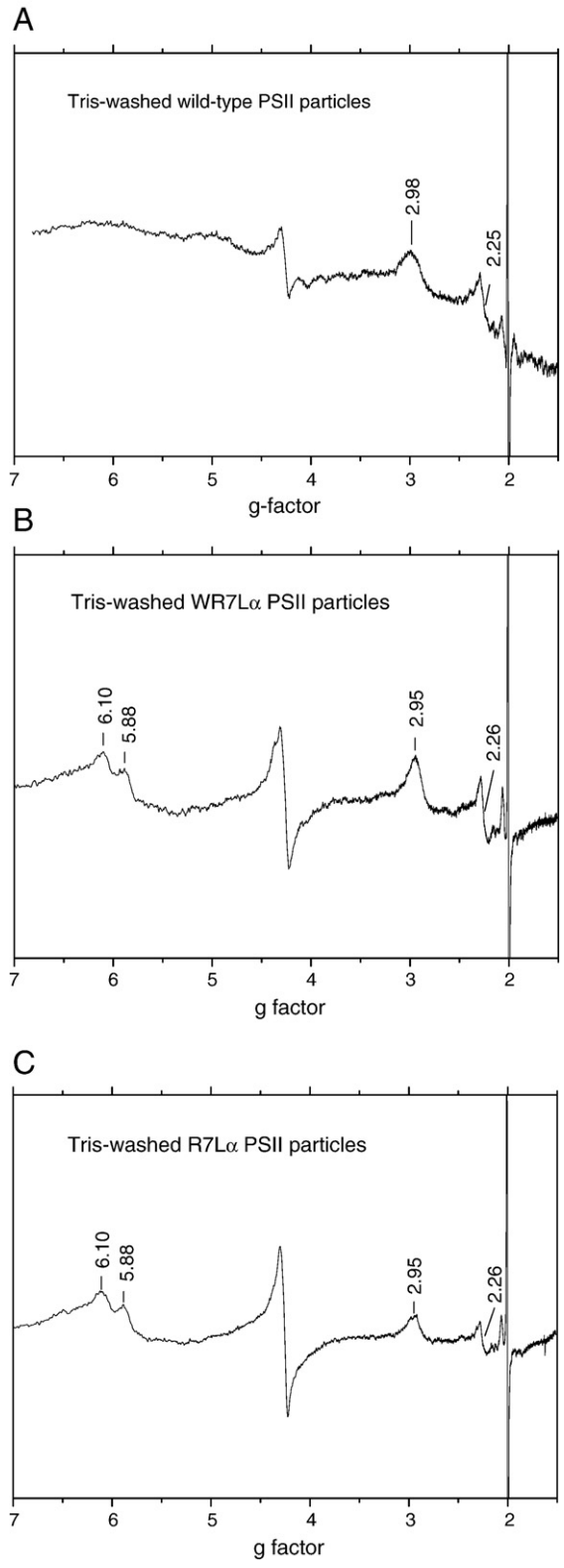

Fig. 11. The EPR spectra of cyt *b559* heme in Tris-washed (A) wild-type, (B) WR7Lα, and (C) R7Lα cyt *b559* mutant PSII core complexes. EPR conditions are the same as in Fig. 10.

Previous studies have identified several spontaneously generated mutants from *Synechocystis* sp. PCC6803 cells and *Chlamydomonas* grown on solid BG-11 medium containing DCMU or other herbicides ([22–24] and references therein). The amino acid side chains involved in herbicide resistance have been mapped in the region of D1 protein between 211 and 275, which constitute the herbicide-binding site [22,23]. In contrast, WR7Lα cyt *b559* mutant cells do not carry any mutation on the D1 protein. In addition, our results in Fig. 6 showed that the inhibitory effect of DCMU concentration on the oxygen-evolving activity of WR7Lα cyt *b559* mutant cells was the same as that of wild-type cells. Therefore, there was no significant mutation-induced structural alteration of the DCMU binding in WR7Lα cyt *b559* mutant cells.

On the other hand, our 77 K fluorescence results, in Fig. 7, showed that the energy transfer from phycobilisomes to the PSII reaction center were partially inhibited or uncoupled in WR7Lα mutant cells. Since DCMU-induced oxidative stress is generated from light-induced charge recombination between radical pairs $P680^+Pheo^-$ in the reaction center, therefore, partially uncoupling the energy transfer from the antenna to the reaction center in WR7Lα mutant cells would dissipate a significant amount of light energy in the antenna and thus decrease possible damage to the PSII reaction center by herbicide-induced photo-oxidative stress.

In addition, WR7Lα mutant cells showed a very distinct chlorophyll *a* fluorescence induction and recovery spectrum at 295 K, compared to wild-type cells (see Fig. 1). The high F_0 value and the increase of the F_M value during actinic light illumination can be attributed to the increased fluorescence emission from uncoupled phycobilisomes in WR7Lα cyt *b559* mutant cells. Therefore, our 295 K chlorophyll *a* fluorescence results are consistent with our 77 K fluorescence results. This distinct pattern in the chlorophyll *a* fluorescence induction and recovery spectrum of WR7Lα mutant cells could be a very useful index for identifying cyanobacterial mutant cells with uncoupled phycobilisomes.

Moreover, previous studies have predicted possible docking sites for the phycobilisomes on the PSII reaction centers [36–39]. ApcE protein possibly acts as a linker protein attaching the phycobilisomes to PSII, also referred to as "linker core membrane" L_{CM}. ApcE proteins may locate within one of the central allophycocyanin (APC) disks of the base cylinders, which may interact with the stromal surface of PSII [36–39]. The proposed docking site for the APC core complex on PSII is in a low protein density area between the CP43, D2 and cyt *b559* [37]. The α-subunit of cyt *b559* is located within or near the predicted contact sites for the APC core complex. Therefore, we propose that this Arg7Leu mutation on the α-subunit of cyt *b559* may alter the interaction of the APC core complex with the PSII reaction center and thus protect mutant cells from DCMU-induced photo-oxidative stress.

Another possibility is that the cyt *b559* in WR7Lα cyt *b559* mutant cells might have greater protective capability under DCMU-induced oxidative stress conditions than that in wild-type cells. However, our results in Fig. 4 show that WR7Lα cyt *b559* mutant cells were more susceptible to photoinhibition than wild-type cells. Therefore, we think that this possibility is less likely, although we cannot completely rule it out at this stage.

A previous study using spectrophotometric redox titration reported that oxygen-evolving wild-type PSII core complexes from *Synechocystis* PCC6803 contain 45% HP form (E_m = 312 mV at pH 6.0) and 55% IP form (E_m = 212 mV at pH 6.0) [40]. The same study also reported that Tris-washed wild-type PSII core complexes contain 5% HP form (E_m > 300 mV at pH 6.0) and 95% IP form (E_m = 178 mV at pH 6.0); after reduction during the course of titration, Tris-washed wild-type PSII core complexes contain 34% IP form (E_m = 235 mV at pH 6.0) and 66% LP form (E_m = 51 mV at pH 6.0) [40]. Our four-step titration results showed that oxygen-evolving wild-type PSII core complexes contain 8% HP form, 78% IP form and 14% LP form of cyt *b559*; Tris-washed wild-type PSII core complexes contain 11% HP form, 59% IP form and 30% LP form of cyt *b559* (see Figs. 9, 10 and Table 2). Therefore, the variations between their results [40] and ours are presumably due to the differences in redox titration methods and experimental conditions [41]. In addition, another previous study reported that they were unable to detect any HP form of cyt *b559* on thylakoid membranes and PSII enriched membranes isolated from

Synechocystis 6803 [42]. Their results suggested that the HP form of cyt *b559* in PSII membranes of *Synechocystis 6803* is labile as compared to other cyanobacteria and higher plants [42]. Furthermore, our results showed that oxygen-evolving and Tris-washed wild-type PSII core complexes contain comparable amounts of HP form (see Table 2). One recent study reported that on Tris-washed spinach PSII membranes, IP form of cyt *b559* was converted into 60% LP and 33% HP forms by the removal of oxygen [41]. We suspect that a similar process might partially occur on Tris-washed *Synechocystis 6803* PSII samples under our experimental conditions. Moreover, our results show that WR7Lα and R7Lα cyt *b559* mutant PSII core complexes (Fig. 8B and C) contain more LP form (~68% and 75%, respectively) of cyt *b559* than oxygen-evolving or Tris-washed wild-type PSII core complexes (~14% and 30%, respectively). The redox forms of cyt *b559* have been explained by changes in the electrostatic environment and/or hydrogen bonding to the heme that tune the *E*m of the heme [5–9,43,44]. Therefore, our results suggest that the electrostatic environment and/or hydrogen bonding to the heme of cyt *b559* are very likely altered in WR7Lα and R7Lα cyt *b559* mutant PSII reaction centers.

Furthermore, we observed EPR signals for the high-spin form of cyt *b559* ($g_z = 6.10$; $g_y = 5.88$) in spectra of WR7Lα and R7Lα cyt *b559* mutant PSII core complexes. These EPR signals of the high-spin form of cyt *b559* were also observed in EPR spectra of H22Kα mutant PSII core complexes (Chu et al., manuscript in preparation) and in PSII membranes treated with 2,3-dichloro-5,6-dicyano-*p*-benzoquinone (characterized with the g = 6.19 and g = 5.95 split signal) [35]. This prior study [35] attributed these high-spin heme EPR signals to the distortion of the axial symmetry of the molecular field by the displacement of one of its histidine axial ligands. It is generally believed that the high-spin state (S=5/2) corresponds to a five-coordinate complex of Fe^{III}PorL, which has a square pyramidal structure where the Fe (III) ion is above the plane of the porphyrin ([35] and references therein). Most six-coordinate octahedral $Fe^{III}PorL_2$ complexes have low spin (S=1/2) ([35] and references therein). Therefore, the EPR signal for the high-spin form of cyt *b559* ($g_z = 6.10$; $g_y = 5.88$) in spectra of WR7Lα and R7Lα cyt *b559* mutant PSII core complexes indicates the displacement of one of the two axial histidine ligands to the heme of cyt *b559* in a significant fraction of their reaction centers. In the recent 2.9 Å PSII crystal structural model [4], the side chain of this Arg residue on the α-subunit of cyt *b559* is in close contact with one of the heme propionates of cyt *b559*. Numerous studies have suggested that the heme propionates are not only simple electrostatic binding anchors, but might also play an active role in regulating electron transfer and biochemical properties of the heme ([45,46] and references therein). Therefore, this Arg7Leu mutation on the α-subunit of cyt *b559* is expected to disrupt the electrostatic interaction between the α-subunit of cyt *b559* and the heme, and thus perturb the structure and electronic properties of the heme in cyt *b559*.

Finally, our results show that the WR7Lα cyt *b559* mutant spontaneously occurred from and outgrew *Synechocystis* sp. PCC6803 wild-type cells in BG-11 medium containing 5 mM Glu and 10 μM DCMU. Therefore, people should be aware of the effects of DCMU-induced photo-oxidative stress while growing *Synechocystis* sp. PCC6803 mutant cells under these conditions.

Acknowledgments

We are grateful to the reviewers for their helpful comments on the manuscript. This work was supported by National Science Council NSC 97-2627-M-001-001, and NSC 96-231-B-001-040-MY3, and Academia Sinica to H.A.C.

References

[1] J. Kern, G. Renger, Photosystem II: structure and mechanism of the water: plastoquinone oxidoreductase, Photosyn. Res. 94 (2007) 183–202.
[2] B. Loll, J. Kern, W. Saenger, A. Zouni, J. Biesiadka, Towards complete cofactor arrangement in the 3.0 Å resolution structure of photosystem II, Nature 438 (2005) 1040–1044.
[3] K.N. Ferreira, T.M. Iverson, K. Maghlaoui, J. Barber, S. Iwata, Architecture of the photosynthetic oxygen-evolving center, Science 303 (2004) 1831–1838.
[4] A. Guskov, J. Kern, A. Gabdulkhakov, M. Broser, A. Zouni, W. Saenger, Cyanobacterial photosystem II at 2.9-Å resolution and the role of quinones, lipids, channels and chloride, Nature Struct. Biol. and Mol. Biol. 16 (2009) 334–342.
[5] D.H. Stewart, G.W. Brudvig, Cytochrome *b559* of photosystem II, Biochim. Biophys. Acta 1367 (1998) 63–87.
[6] O. Kaminskaya, J. Kurreck, K.D Irrgang, G. Renger, V.A. Shuvalov, Redox and spectral properties of cytochrome *b559* in different preparations of photosystem II, Biochemistry 38 (1999) 16223–16235.
[7] M. Roncel, A. Boussac, J.L. Zurita, H. Bottin, M. Sugiura, D. Kirilovsky, J.M. Ortega, Redox properties of the photosystem II cytochrome *b559* and *c550* in the cyanobacterium *Thermosynechococcus elongates*, J. Biol. Inorg. Chem. 8 (2003) 206–216.
[8] O. Kaminskaya, J. Kern, V.A. Shuvalov, G. Renger, Extinction coefficients of cytochromes *b559* and *c550* of *Thermosynechococcus elongates* and Cyt *b559*/PSII stoichiometry of higher plants, Biochim. Biophys. Acta 1708 (2005) 333–341.
[9] T. Shibamoyo, Y. Kato, T. Watanabe, Spectroelectrochemistry of cytochrome *b559* in the D1–D2–Cyt *b559* complex from spinach, FEBS Lett. 582 (2008) 1490–1494.
[10] G. Barber, J. De Las Rivas, A functional model for the role of cytochrome b_{559} in the protection against donor and acceptor side photoinhibition, Proc. Natl. Acad. Sci. U. S. A. 90 (1993) 10942–10946.
[11] C.A. Tracewell, G.W. Brudvig, Characterization of the secondary electron-transfer pathway intermediates of photosystem II containing low-potential cytochrome *b559*, Photosynth. Res. (2008) 189–197.
[12] J. Kruk, K. Strzalka, Dark reoxidation of the plastoquinone-pool is mediated by the low-potential form of cytochrome *b559* in spinach thylakoids, Photosynth. Res. 62 (1999) 273–279.
[13] J. Kruk, K. Strzalka, Redox changes of cyt *b559* in the presence of plastoquinones, J. Biol. Chem. 276 (2001) 86–91.
[14] N. Bondarava, L. De Pascalis, S. Al-Babili, C. Goussias, J.R. Golecki, P. Beyer, R. Bock, A. Krieger-Liszkay, Evidence that cytochrome *b559* mediates the oxidization of reduced plastoquinone in the dark, J. Biol. Chem. 278 (2003) 13554–13560.
[15] O. Kaminskaya, V.A. Shuvalov, G. Renger, Evidence for a novel quinone-binding site in the photosystem II (PSII) complex that regulates the redox potential of cytochrome *b559*, Biochemistry (2007) 1091–1105.
[16] O. Kaminskaya, V.A. Shuvalov, G. Renger, Two reaction pathway for transformation of high potential cytochrome *b559* of PSII into the intermediate potential form, Biochim. Biophys. Acta 1767 (2007) 550–558.
[17] A. Trebst, Inhibitors in the functional dissection of photosynthetic electron transport system, Photosynth. Res. 92 (2007) 217–224.
[18] A.W. Rutherford, A. Krieger-Liszkay, Herbicide-induced oxidative stress in photosystem II, Trend Biochem. Sci. 26 (2001) 648–653.
[19] C. Fufezan, A.W. Rutherford, A. Krieger-Liszkay, Singlet oxygen production in herbicide-treated photosystem II, FEBS Lett. 532 (2002) 407–410.
[20] A. Krieger-Liszkay, Singlet oxygen production in photosynthesis, J. Exp. Bot. 56 (2005) 337–346.
[21] M. Ikeuchi, S. Tabata, *Synechocystsis* sp. PCC6803 — a useful tool in the study of genetics of cyanobacteria, Photosyn. Res. 70 (2001) 73–83.
[22] J. Hirschberg, A.B. Yehuda, I. Pecker, N. Ohad, Mutations resistant to photosystem II herbicides, in: D.V. Wettstein, N. Chua (Eds.), Plant Molecular Biology, 1987, pp. 357–366, Plenum press, New York.
[23] Y. Narusaka, M. Narusaka, H. Kobayashi, K. Satoh, The herbicide-resistant species of the cyanobacterial D1 protein obtained by thorough and random in vitro mutagenesis, Plant Cell Physiol. 39 (1998) 620–626.
[24] W. Oettmeier, Herbicide resistance and supersensitivity in photosystem II, Cell Mol. Life Sci. 55 (1999) 1255–1277.
[25] C.-H. Hung, J.-Y. Huang, Y.-F. Chiu, H.-A. Chu, Site-directed mutagenesis on the heme axial-ligands of cytochrome *b559* in photosystem II by using cyanobacteria *Synechocystis* PCC 6803, Biochim. Biophys. Acta 1767 (2007) 686–693.
[26] H.-A. Chu, A.P. Nguyen, R.J. Debus, Site-directed photosystem II mutants with perturbed oxygen-evolving properties. 1. Instability or inefficient assembly of the manganese cluster *in vivo*, Biochemistry 33 (1994) 6137–6149.
[27] H.M. Gleiter, E. Haag, J.-R. Shen, J.J. Eaton-Rye, Y. Inoue, W.F.J. Vermaas, G. Renger, Functional characterization of mutant strains of the cyanobacterium *Synechocystis* sp. PCC6803 lacking short domains within the large, lumen-exposed loop of chlorophyll protein CP47 in photosystem II, Biochemistry 33 (1994) 12063–12071.
[28] P.J. Nixon, B.A. Diner, Aspartate 170 of the photosystem II reaction center polypeptide D1 is involved in the assembly of the oxygen-evolving manganese cluster, Biochemistry 31 (1992) 942–948.
[29] H.B. Pakrasi, B.A. Diner, J.G.K. Williams, C.J. Arntzen, Deletion mutagenesis of the cytochrome *b559* protein inactivates the reaction center of photosystem II, Plant Cell 1 (1989) 591–597.
[30] G. AjLani, G. Vernotte, L. DiMagno, R. Haselkorn, Physobilisome core mutants of *Synechocystis* PCC 6803, Biochim. Biophys. Acta 1231 (1995) 189–196.
[31] V.A. Dzelzkalns, L. Bogorad, Spectral properties and composition of reaction center and ancillary polypeptide complexes of photosystem II deficient mutants of *Synechocystis* 6803, Plant Physiol. 90 (1989) 617–623.
[32] G. Ajlani, C. Vernotte, Construction of a phycobiliprotein-less mutant of *Synechocystis* sp. PCC 6803, Plant Mol. Biol. 37 (1998) 577–580.

[33] E. Haag, J.J. Eaton-Rye, G. Renger, W.F.J. Vermaas, Functionally important domains of the large hydrophilic loop of CP47 as probed by oligonucleotide-directed mutagenesis in *Synechocystis* sp. PCC 6803, Biochemistry 32 (1993) 4444–4454.
[34] K.V. Lakshmi, M.J. Reifler, D.A. Chisholm, J.Y. Wang, B.A. Diner, G.W. Brudvig, Correlation of the cytochrome *c550* content of cyanobacterial photosystem II with the EPR properties of the oxygen-evolving complex, Photosyn. Res. 72 (2002) 175–189.
[35] T.N. Kropacheva, W.O. Feikema, F. Mamedov, Y. Feyziyev, S. Styring, A.J. Hoff, Spin conversion of cytochrome *b559* in photosystem II induced by exogenous high potential quinine, Chemical Physics 294 (2003) 471–482.
[36] D. Bald, J. Kruip, M. Rögner, Supramolecular architecture of cyanobacterial thylakoid membranes: How is the phycobilisome connected with the photosystem? Photosynth. Res. 49 (1996) 103–118.
[37] J. Barber, E.P. Morris, P.C.A. da Fonseca, Interaction of allophycocyanin core complex with photosystem II, Photochem. Photobiol. Sci. 2 (2003) 536–541.
[38] C. Büchel, W. Kühlbrandt, Structural difference in the inner part of photosystem II between higher plants and cyanobacteria, Photosyn. Res. 85 (2005) 3–13.
[39] C.W. Mullineaux, Phycoblisome-reaction center interaction in cyanobacteria, Photosynth. Res. 95 (2008) 175–182.
[40] D.H. Stewart, G.W. Brudvig, A new model of cytochrome *b559* function based on the observation of a reversible redox-linked interconversion between two redox forms of cytochrome b559. In: Garab G. (ed) Photosynthetic Mechanism and Effects, vol 2. Kluwer Academic Publishers, Dordrecht, The Netherlands, pp 1113–1116.
[41] F. Mamedov, R. Gadjieva, S. Styring, Oxygen-induced changes in the redox state of the cytochrome *b559* in photosystem II depend on the integrity of the Mn cluster, Physiol. Plant. 131 (2007) 41–49.
[42] J.M. Ortega, H. Manuel, A. Miguel, M. Roncel, M. Losada, Redox properties of cytochrome *b559* in photosynthetic membranes from the cyanobacterium *Synechocystis* sp. PCC 6803, J. Plant. Physiol. 144 (1994) 454–461.
[43] C. Berthomieu, A. Boussac, W. Mantele, J. Breton, E. Nabedryk, Molecular changes following oxidoreduction of cytochrome *b559* characterized by Fourier transform infrared difference spectroscopy and electron paramagnetic resonance, Biochemistry 31 (1992) 11460–11471.
[44] M. Roncel, J.M. Ortega, M. Losada, Factors determining the special redox properties of photosynthetic cytochrome *b559*, Eur. J. Biochem. 268 (2001) 4961–4968.
[45] V. Guallar, B. Olsen, The role of the heme propionates in heme biochemistry, J. Inorg. Biochem. 100 (2006) 755–760.
[46] D.A. Mills, L. Geren, C. Hiser, B. Schmidt, B. Durham, F. Millett, S. Ferguson-Miller, An arginine to lysine mutation in the vicinity of the heme propionates affects the redox potentials of the hemes and associated electron and proton transfer in cytochrome *c* oxidase, Biochemistry 44 (2005) 10457–10465.